Modeling Fibrosis Infiltration in a Virtual Cohort: Impact on Atrial Fibrillation Vulnerability

Giada S Romitti, María Termenón-Rivas, Alejandro Liberos, Miguel Rodrigo

Computational Multiscale Simulation Lab (CoMMLab), Department of Computer Science and Department of Electronic Engineering, Universitat de València, València, Spain

Abstract

Atrial fibrillation (AF) is a growing clinical challenge, with computational modeling proving valuable for understanding its mechanisms and guiding personalized therapies. In this study, we used a virtual cohort of 10 bi-atrial geometries to investigate how different fibrosis modeling strategies affect AF vulnerability. We introduced a method to generate fibrotic patterns aligned with myocardial fiber orientation and incorporated TGF-β1-mediated remodeling into the Koivumäki atrial model to simulate structural and electrical changes. A total of 200 simulations were performed across multiple pacing sites and fibrosis conditions. Without fibrosis, AF was induced in only 22% of simulations, highlighting the role of fibrotic remodeling. The decoupling with ionic remodeling (D+IR) model yielded realistic arrhythmia rates (~46%) without parameter tuning. The anisotropy with ionic remodeling model (IA+IR) required additional diffusion adjustments to reach ~26%, while the decoupling model (D) alone led to unrealistically high inducibility (~60%). LA pacing, particularly near the RPVs, was most arrhythmogenic (~67%) compared to RA sites. These findings highlight the importance of fibrosis representation and pacing location in AF modeling and support the D+IR approach as a strong candidate for personalized simulations.

1. Introduction

Atrial fibrillation (AF) is the most common sustained arrhythmia, with its prevalence rising by over 30% in the past two decades and expected to grow further [1]. Computational modeling, particularly through virtual cohorts and digital twin technologies, offers new opportunities for improving AF diagnoses, prognoses, and treatments personalization [2].

Among the key pro-arrhythmic features, atrial fibrosis plays a central role by altering conduction and promoting reentrant activity [3]. To accurately reflect the patient-specific nature of AF, it is essential to integrate realistic fibrotic remodeling into computational models [4, 5].

In this study, we use a virtual population of bi-atrial geometries to explore how different fibrosis modeling strategies affect AF vulnerability. We propose a novel technique for generating fibrotic patches aligned with myocardial fibers orientation and adapt the Koivumäki atrial cellular model to simulate TGF-β1-induced remodeling. By running simulations across different pacing sites and fibrosis configurations, we quantify how modeling choices influence AF vulnerability, advancing the development of more personalized and predictive cardiac models.

2. Material and Methods

2.1. Fibrosis Assignment Algorithm

To simulate the spatial distribution of fibrosis in atrial tissue aligned with the myocardial fibers, we developed a custom algorithm that iteratively expands fibrotic regions from a set of initial seed nodes $S = \{\boldsymbol{s}_1, \boldsymbol{s}_2, \dots, \boldsymbol{s}_n\}$. At each step, the algorithm evaluates the fiber direction $\boldsymbol{F}_i$ at a given node $\boldsymbol{v}_i$ and introduces a probabilistic rule for fibrosis propagation based on the angle between local fiber direction and neighboring node $\boldsymbol{v}_j \in N(\boldsymbol{v}_i)$ vectors.

Additionally, two parameters are considered: a global grade of directionality (*grDir*) and a global grade of aleatoriety (*grAle*). The former regulates how strongly the local fiber orientation influences fibrosis propagation, while the latter introduces stochastic variability into the spread.

The process continues until the total amount of fibrosis reaches a predefined threshold $percLim$, calculated as:

$$P = \frac{\sum f(\boldsymbol{v}_i)}{N_{nodes}}$$

where $f(\boldsymbol{v}_i) = 1$ if the node is fibrotic, and $f(\boldsymbol{v}_i) = 0$ otherwise. A schematic overview of this procedure is shown in Figure 1.

2.2. Computational Domains

N = 10 bi-atrial geometries were extracted from a larger dataset constructed using Statistical Shape Modeling (SSM) techniques [6]. Each was remeshed into a fine tetrahedral mesh with an average spatial resolution of 0.5 mm, yielding 644,240 ± 75,155 vertices and 3,642,000 ± 425,150 elements per geometry. To preserve anatomical accuracy, original tissue classifications and fiber orientations from the SSM dataset were retained in all remeshed models (Figure 2A).

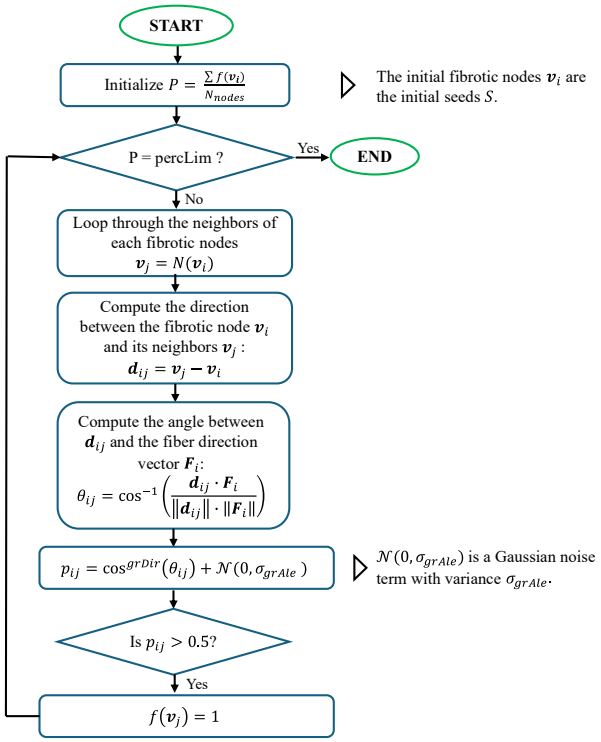

Figure 1. Flowchart describing fibrosis distribution algorithm.

2.3. Fibrotic Substrate Modeling

To model the fibrotic substrate, we implemented three distinct approaches, referred to as: decoupling (D), decoupling with ionic remodeling (D+IR), and increased anisotropy with ionic remodeling (IA+IR).

In the D model, fibrotic nodes were modeled as electrically non-conductive tissue by assigning null diffusion (D = 0 S/m), effectively simulating complete myocyte decoupling.

The D+IR model, as proposed by [5], included both structural decoupling (achieved by randomly decoupling 30% of the fibrotic nodes) and ionic remodeling induced by transforming growth factor β1 (TGF-β1), reflecting inflammation-driven electrophysiological changes [7]. The specific ionic modifications are summarized in Table 1, with the corresponding transmembrane voltage (TV) trace shown in Figure 2B. These changes led to a 23.98% increase in APD, a 38.06% reduction in upstroke velocity, and a 2.56% shift in resting membrane potential, evaluated in a 2D simulation (0.3 x 2 x 0.025 cm, 2106 nodes), compared with the persistent AF (PsAF) cellular model.

The IA+IR model, based on [4], incorporated TGF-β1–mediated ionic remodeling together with increased anisotropy, implemented as a 2:1 ratio of longitudinal to transverse conduction velocities. Baseline conduction properties used across all models, including the initial anisotropy ratio, were defined according to [11]. Additionally, a complementary analysis was performed for this model to assess the impact of reduced overall conductivity in fibrotic regions, where diffusion values were scaled to 50%, 25%, and 10% of those in non-fibrotic tissue.

Fibrosis extent was identical for each anatomical model and was defined according to the Utah Stage 4 classification, resulting in fibrotic node percentages of 35.9 ± 0.8% in the LA and 15.8 ± 0.5% in the RA, consistent with reported ranges in the literature (>30% in LA, 5–20% in RA) [8] (Figure 2C).

Table 1. Multiplying factors to maximum ionic conductance.

	Healthy	PsAF	TGF-β1
g_{K1}	1.00	2.00	1.40
g_{Ks}	1.00	1.00	2.00
g_{CaL}	1.00	0.40	0.18
g_{Kur}	1.00	0.80	0.80
g_{to}	1.00	0.56	0.56
g_{Na}	1.00	1.00	0.60

2.4. Simulations Framework

Atrial biophysical simulations were conducted using the Koivumäki et al. cellular model [9], implemented within the monodomain model. Simulations used a GPU-accelerated finite element solver [10] with a fixed time step of 20 µs. Nodes were classified as fibrotic or non-fibrotic. Non-fibrotic nodes were assigned a 100% electrical remodeling profile, representative of PsAF with shortened action potential (APD_{90}(2 Hz) = 103 ms) respect to the healthy model (APD_{90}(2 Hz) = 240 ms) [11]. The resulting TV traces are shown in Figure 2B.

AF inducibility was tested using a pacing protocol at five stimulus location (three in the LA, two in the RA), located near fibrotic regions (Figure 2D) [12]. Pacing followed a progressively shortening cycle length (from 400 ms down to 140 ms). AF was considered induced if electrical activity persisted for at least five seconds following the final pacing stimulus. In total, 200 simulations were performed across 10 patient geometries, 4 models (no fibrosis, D, D+IR, IA+IR), and 5 stimulation sites.

3. Results

3.1. Fibrotic Substrate Modeling

Figure 3A shows voltage maps comparing the IA+IR fibrotic model under two different diffusion settings: healthy diffusion (100%) and reduced diffusion (25%) within fibrotic regions. Whereas considering original diffusion (100%) the wave propagation is not affected by the fibrosis presence, lower diffusion values (25%) exhibits conduction discontinuities and wave-breaks, which are known precursors to reentrant activity and AF initiation. Conduction velocity maps (Figure 3B) highlight that the 25% diffusion case yields longitudinal CV values in agreement with previous experimental data (20 cm/s) [4], supporting the physiological relevance of this parameter choice. Additional simulations in two representative geometries (Figure 3C–D) demonstrate that in the absence of diffusion downscaling, no arrhythmic activity could be initiated.

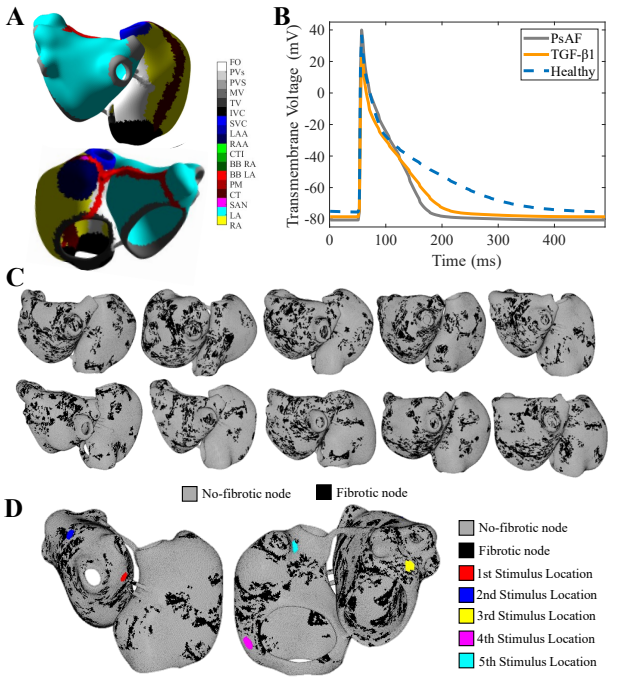

Figure 2. (A) Representative atrial geometry with tissue types. (B) Transmembrane voltage traces for healthy (blue), PsAF (grey), and fibrotic (orange) tissue conditions. (C) Bi-atrial geometries employed with their fibrosis distribution. (D) Atrial anatomy with non-fibrotic (grey) and fibrotic (black) regions, and the five stimulation sites.

3.2. Arrhythmic Vulnerability

The results of our arrhythmic vulnerability analysis, through the whole database, are summarized in Figure 4. Panel (A) displays the percentage of arrhythmic cases based on the model of fibrosis used. When fibrosis is not integrated, 22±32 % of arrhythmic cases are observed. The decoupling model shows the highest vulnerability, with 60±30% of cases, followed by the D+IR model, which reaches 46±33% and the IA+IR model with 26 ± 25%.

Panel (B) presents the percentage of arrhythmic cases according to the stimulus location. LA sites were generally more arrhythmogenic, with the region between the right pulmonary veins (RPVs) showing the highest vulnerability at 67% on average. Overall, LA stimulation led to arrhythmia in 48% of cases, compared to 24% for RA sites.

Finally, across all locations and models, arrhythmias were induced in $37.7 \pm 22.2\%$ of cases, highlighting notable variability across models and patients. Nonetheless, the D and D+IR models consistently showed higher arrhythmic vulnerability.

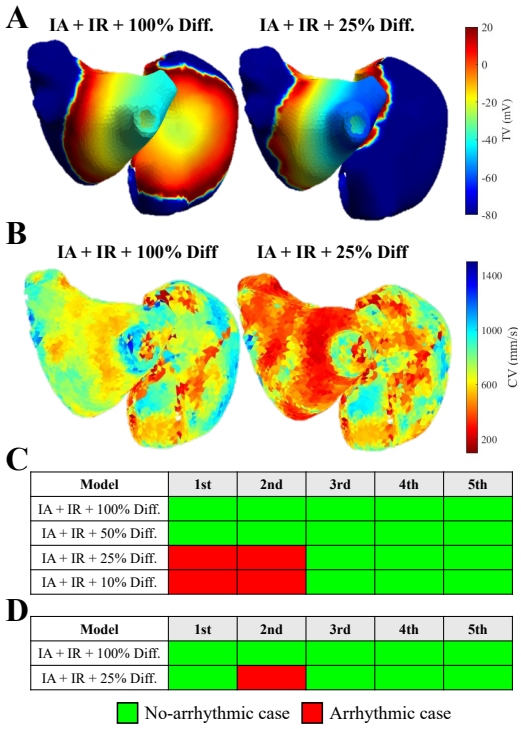

Figure 3. (A) Transmembrane voltage (TV) maps and (B) conduction velocity (CV) maps comparing the IA+IR model with 100% diffusion (left) versus 25% diffusion (right). Arrhythmic versus non-arrhythmic outcomes for two different virtual patient shown in (C) and (D) under different stimulus location using the IA+IR model with varying diffusion levels in fibrotic areas.

4. Discussion and Conclusions

In this study, we developed a fast and biologically informed algorithm to generate fibrotic patterns aligned

with myocardial fiber directions. Combined with the integration of TGF-β1 effects into the Koivumäki model, this allowed us to simulate both structural and electrophysiological remodeling with realistic biomarker output [4]. We conducted 200 simulations across four fibrosis definitions (no fibrosis, D, D+IR, IA+IR) to assess their impact on arrhythmia vulnerability. Without fibrosis, only 22% of cases resulted in arrhythmia, highlighting the essential role of fibrotic remodeling. This level of inducibility is expected, as the baseline model includes a PsAF degree of electrical remodeling.

The D model showed the highest inducibility (~60%) but likely overestimates arrhythmic risk due to excessive node disconnection. The IA+IR model required diffusion tuning to sustain reentry, highlighting sensitivity to solver, mesh, or cell model. This limits reproducibility across frameworks. In contrast, the D+IR model [5] yielded realistic arrhythmia rates without parameter tuning, offering more physiologically consistent results.

We also found that left atrial pacing was significantly more arrhythmogenic than right atrial, especially near the right pulmonary veins (67% inducibility), in accordance with the higher fibrosis infiltration in LA respect to RA.

We plan to expand this study with a larger virtual cohort, more Utah fibrosis stages, and additional pacing sites. Future work will also explore how variations in fibrosis parameters (grDir, grAle) affect pattern formation, potentially capturing greater patient-specific heterogeneity. This will strengthen the robustness and personalization of arrhythmia risk assessment.

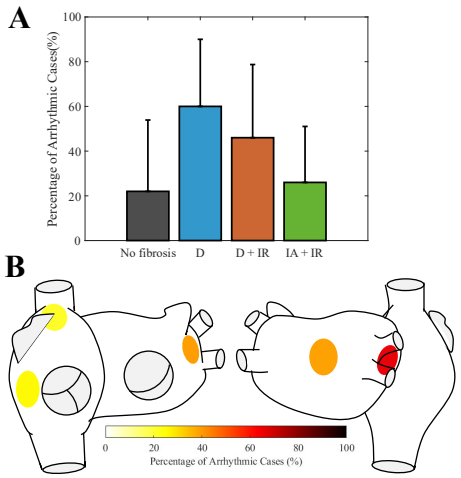

Figure 4. (A) Percentage of arrhythmic cases depending on the type of model used. (B) Mean percentage of arrhythmic cases depending on the stimulus location.

Acknowledgments

This work was funded by Generalitat Valenciana Grant AICO/2021/318 (Consolidables 2021), Grants PID2020-114291RB-I00, PID2023-148702OB-I00 and EraNet PCI2024-153442 funded by MCIN/ 10.13039/501100011033 and by "ERDF A way of making Europe".

References

[1] G. Lippi et al., "Global epidemiology of atrial fibrillation: an in-creasing epidemic and public health challenge," *International Journal of Stroke*, vol. 16, no. 2, pp. 217-221, 2021.

[2] S. A. Niederer et al., "Creation and application of virtual patient cohorts of heart models," *Philosophical Transactions of the Royal Society A*, vol. 378, no. 2173, 2020.

[3] B. Burstein et al., "Atrial fibrosis: mechanisms and clinical relevance in atrial fibrillation," *Journal of the American College of Cardiology*, no. 51, vol. 8, pp. 802-809, 2008.

[4] J. B. Hakim et al., "Arrhythmia dynamics in computational models of the atria following virtual ablation of re-entrant drivers," *EP Europace*, vol. 20, no. suppl_3, pp. iii45-iii54, 2018.

[5] P. Martinez Díaz et al., "The right atrium affects in silico arrhythmia vulnerability in both atria," *Heart Rhythm*, vol. 21, no. 6, pp. 799-805, 2024.

[6] C. Nagel et al., "A bi-atrial statistical shape model and 100 volumetric anatomical models of the atria [Data set]," *Zenodo*. https://doi.org/10.5281/zenodo.5004620, 2021.

[7] C. H. Roney et al., "Modelling methodology of atrial fibrosis affects rotor dynamics and electrograms. *EP Europace*, vol. 18, no. suppl_4, pp. iv146-iv155, 2016.

[8] N. Akoum et al., "Atrial fibrosis quantified using late gadolinium enhancement MRI is associated with sinus node dysfunction requiring pacemaker implant," *Journal of Cardiovascular Electrophysiology*, vol. 23, no. 1, pp. 44-50, 2012.

[9] J. T. Koivumäki et al., "In silico screening of the key cellular remodeling targets in chronic atrial fibrillation," *PLoS Computational Biology*, vol. 10, no. 5, 2014.

[10] V. García-Mollá et al., "Adaptive step ODE algorithms for the 3D simulation of electric heart activity with graphics processing units," *Computers in Biology and Medicine*, vol. 44, pp. 15-26, 2014.

[11] G. S. Romitti et al., "Implementation of a cellular automaton for efficient simulations of atrial arrhythmias," *Medical Image Analysis*, pp. 103484, 2025.

[12] P. M. Boyle et al., "Characterizing the arrhythmogenic substrate in personalized models of atrial fibrillation: sensitivity to mesh resolution and pacing protocol in AF models," *EP Europace*, vol. 23, no. suppl_1, pp. i3-i11, 2021.

Address for correspondence:

Miguel Rodrigo Bort
Av. de l'Universitat, s/n. 46100, Burjassot (Valencia, Spain).
miguel.rodrigo@uv.es